

Analysis of Subsurface Geological Structure Using Magnetotelluric Data

Wambra Aswo Nuqramadha^{1,2}, Yunus Daud^{1,2}, Fikri Fahmi¹, Ahmad Zarkasyi³, Asep Sugiyanto³, Edi Suhanto³

¹PT . NewQuest Geotechnology, Indonesia

²Master Program in Geothermal Exploration, Graduate Program of Physical Science, The University of Indonesia

³Center for Geological Resources, Geological Agency, Indonesia

wam.aswo@gmail.com

Keywords: MT, subsurface, geological structure, geothermal system

ABSTRACT

Exploration stage still holds the biggest challenge and has a high risk in the geothermal industry. Therefore, it requires a good understanding of subsurface conditions by integrating high quality geoscientific data. The main goal of exploration is the determination of drilling target. The subsurface drilling target is actually directed to high temperature and high permeability zone. Subsurface temperature distribution could be approximated based on the resistivity values obtained from MT data, while the zones with high permeability are associated with geological structures. Geological mapping could only figure out geological structures indicated at the surface. However, continuation of the geological structure into the subsurface is difficult to detect. This study focused on the identification of subsurface geological structure using Magnetotelluric (MT) data. Analysis of splitting pattern from MT curve, the orientation elongation of polar diagrams, as well as delineation of subsurface structures were done by referring to the results of 3-dimensional inversion obtained from MT, which is the method used in this study. Geological data were included as supporting data to make the analysis of the presence of subsurface geological structure become more comprehensive. The final stage of this research is to provide updated structural map confirmed by MT.

1. INTRODUCTION

Exploration in the geothermal industry is the most crucial stages and contains the highest risk. Therefore, developing exploration technology that can reduce the high risk is still a challenge. The main purpose of the exploration is to determine the drilling location. The drilling target should be directed to reservoir zone that has high temperature and high permeability. Temperature associated with the presence of heat source, while permeability associated with the presence of fluid-filled fractures. Temperature distribution has a correlation with the distribution of subsurface resistivity structure (Ussher et al, 2000). Accordingly, distribution of temperature could be represented by subsurface resistivity structure. On the other hand, detection of geological structures with good permeability, requires a more comprehensive method.

The scientific research related to identification of geological structure is only applied in a couple of cases (Tong, et al., 2008; Onacha, 2009). Given the importance of knowing the drilling target with higher level of confidence, this research focused to address the biggest challenge in this exploration phase. The identification process will be done by utilizing MT data, as well as correlating with geological data.

Therefore, it would produce a more comprehensive analysis in identifying “hot and permeable” zones.

2. BASIC CONCEPT

2.1. Vertical Contact Phenomena

Curve splitting of TE (Transverse Electric) and TM (Transverse Magnetic) mode and impedance polarization of MT data is caused by subsurface electrical discontinuity (Figure 1 and Figure 2). The physical principle governing induction at a discontinuity is conservation current. Figure 1 shows a very simple 2-D scenario with a vertical contact between two zones of different conductivity, σ_1 and σ_2 (Simpson & Bahr, 2005). The current density, (j_y), across the boundary is given by:

$$j_y = \sigma E_y \quad (1)$$

Subsurface electrical discontinuity causes discontinuity in electric field (E_y) triggering discontinuity in TM mode. Edge effect causes TM mode is more sensitive to the lateral change than TE mode. However, TE mode is associated with vertical magnetic field influencing sensitivity to the subsurface conductivity. The difference of characteristics causes splitting between TE and TM modes of the vertical contact.

2.2. Curve Splitting Phenomena

Splitting of MT data curve at certain frequency range usually occurs because of vertical contact in the subsurface. Structure located near MT stations, can cause splitting on the MT curves. The splitting pattern really depends on how much impact of the structure towards the MT data. One of the effecting factors is the distance of the structure to the MT station. From the forward modeling result we can see that the closer it is to the structure, the higher the frequency is where splitting occur (Daud at al, 2015)

2.3. Impedance Polar Diagram Phenomena

To determine the existence of a structure, impedance polar diagram of MT data can be analyzed by utilizing impedance data using MT3DMod-X software. Starting from a tensor impedance which is derived from measurements, and assuming 2-D conditions, several different ways have been used to find the rotation angle between measurement direction and strike. One of these is rotation the impedance Z_{ij} in steps, plot them on a polar diagram, and pick an optimum angle from the plots. An optimum angle maximizes or minimizes some combination of the Z_{ij} . These interesting diagrams, called impedance polar diagram, are usually plotted at many frequencies, because in practice the strike direction often changes with depth (Vozzof, 1991).

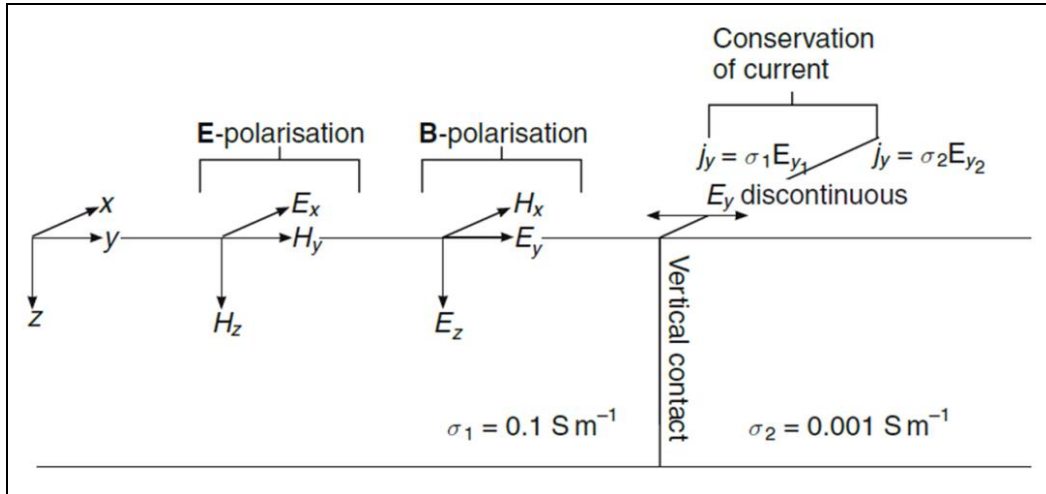


Figure 1. Simple 2-D model composed of quarter-spaces with different conductivities meeting at vertical contact. Conservation of current across the contact, where the conductivity change from σ_1 and σ_2 , leads to the y-component of the electric field, E_y , being discontinuous (Simpson & Bahr, 2005)

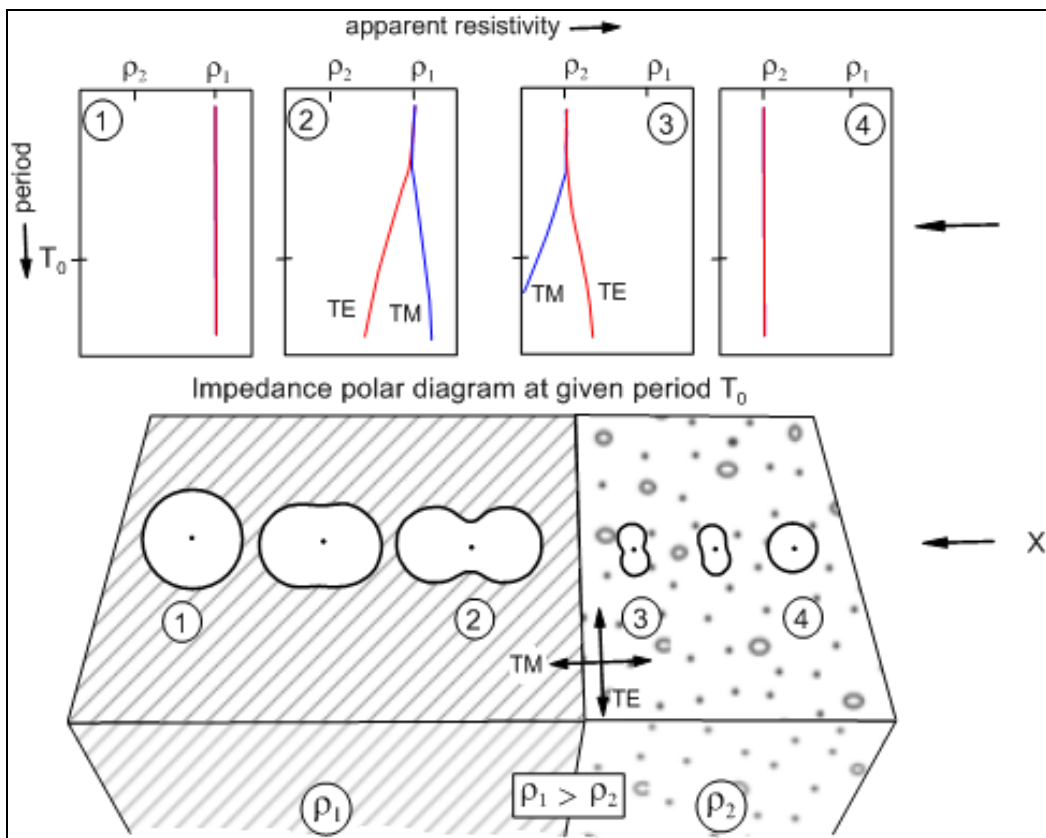


Figure 2. Curve Splitting (above) and impedance polar diagram (below) phenomena at MT station 1, 2, 3 and 4 (Vozzof, 1991)

The elongation of polar diagram could provide information on the strike direction, in which polar diagram of the MT station located at more conductive zone give the response of relatively parallel to the strike, while the polar diagram of the MT station located at more resistive zone give the response of relatively perpendicular to the strike. From this simulation, it can be understood that the location of the fault structure can be detected (Daud et al, 2015).

3. APPLICATION OF THE MT TECHNOLOGY IN GEOTHERMAL PROSPECT AREA

MT technology for detecting subsurface geological structure is applied in a geothermal area. Analysis of splitting curve, elongation of polar diagram, and the result of 3D inversion are used to image the continuity of geological structure in the subsurface. The output of analysis result is structural map that confirmed by MT data.

3.1. Surface Geological Structure

Surface geological structure at the geothermal area is derived from the result of field observation data (Figure 3). Tectonic and volcanic structures exist at the area. Tectonic structures have dominant orientation to NW-SE, NE-SW, and relatively N-S direction. While volcanic structures consist of caldera and volcanic dome. The structures probably influence the development of geothermal system in the area.

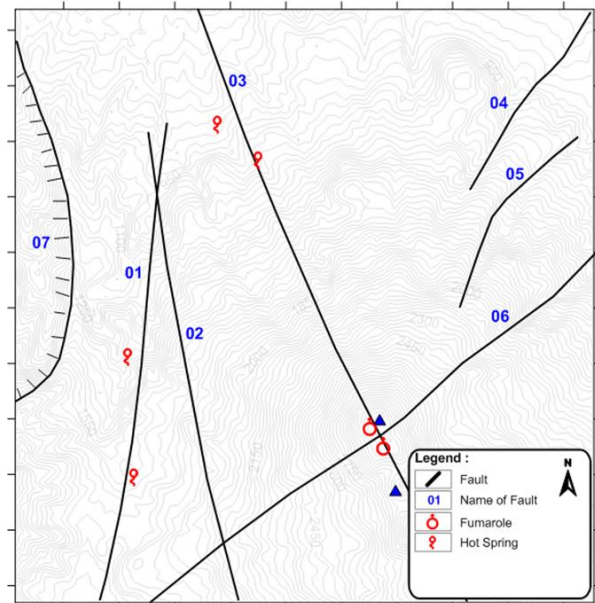


Figure 3. Surface geological structure derived from field observation

3.2. Distribution of MT Data

The MT survey was carried out at 35 stations covering the the geothermal area. The survey was designed with station interval of 500 - 2500 meter. To overcome possible static shift of the MT curve, geostatistic-averaging method was applied, because no TDEM data available at the survey area. Most of MT data have excellent to very good quality.

MT profile that has been made consists of 4 profiles, with distribution as shown at Figure 4. All of the profiles oriented W-E.

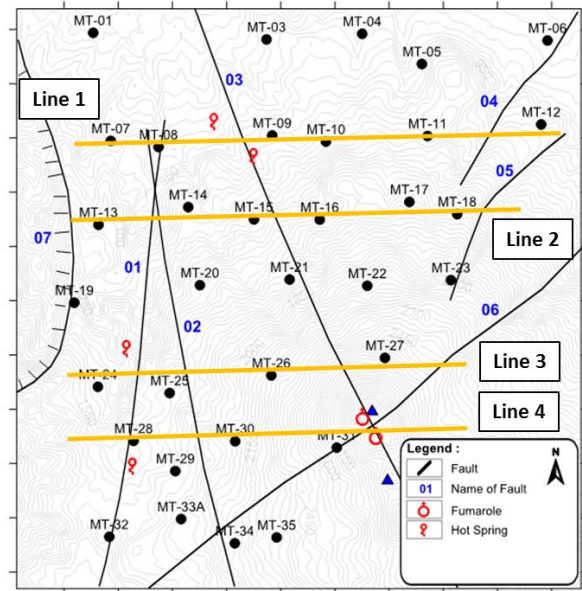


Figure 4. Distribution of MT data and MT profile that will used for structure analysis

3.3. The Result of Analysis

Surface geological structure derived from observation data are identified to be continued to subsurface by analyzing curve splitting, polar diagram and 3D inversion of MT data. Three-dimensional inversion of MT data was done by using MT3Dinv-X software developed by NewQuest Geotechnology (Daud et al, 2012).

Curve Splitting and 3D Inversion Result

Curve splitting and 3D inversion result of Line 1 is shown in **Figure 6**. There are 3 faults of which the continuation could be identified in the subsurface from 3D inversion result (02, 03, 04). The existence of Fault 03 is also detected by MT-09. Splitting curves of MT-11 and MT-12 are possibly caused by Fault 04. However, the existence of Fault 02 is not strongly supported by splitting curve of MT-07, and MT-08, because the splitting pattern is not too significant.

The continuity of Fault 02 and 03 could be seen in Line 2 (**Figure 7**). The slope of the faults are also consistent. The existence of the faults are also supported by splitting curve of MT stations (MT-13, MT-14, MT-15, MT-16). Other fault crossed by Line 2 (05) is also imaged by 3D inversion result. Unfortunately, the existence of faults can not be analyzed by splitting curve, because there is only one MT stations located close to the fault.

In Line 3 (**Figure 8**), the existence of Fault 02 and 03 continue, and are also supported by splitting curve of MT-25, MT-26 and MT-27. There is a new identified fault in Line 3 (Fault 01). The fault could not be identified at the previous lines, because Fault 01 is located close to Fault 02, and no MT data in between of them. The existence of Fault 01 is also indicated by the occurrence of hot spring at the surface. In addition, the indication of Fault 06 could be imaged by MT section of Line 3. Nevertheless, the indication could not be supported by MT data, because of no MT data located close to the fault.

Splitting pattern of MT curves (MT-28, MT-29, MT-30, MT-31) support the existence of Fault 01, 02 and 03 in Line 4 (**Figure 9**). Furthermore, the continuity of Fault 06 also could be identified by the result of 3D inversion. However,

the fault did not plotted in the MT section, because the occurrence of the fault overlaps with Fault 03.

Polar Diagram

The elongation of polar diagrams have general trend relatively to NE-SW and NW-SE direction. The indication can be seen clearly at 0.1 Hz (**Figure 10**). Because the lower frequency give information of deeper (probably dominant) structure. Polar diagrams provide reinforcement to the analysis result of curve splitting and 3D inversion, as well as complete the analysis of faults that are not crossed by the inversion line. The identified faults, such as Fault 01, 02, 03, 04 and 05, are reinforced by elongation of polar diagram. The elongation generally paralel to the fault. Polar diagrams also support to identify the faults that are not clear enough from curve splitting and 3D inversion, such as Fault 06. Direction of Fault 06 is informed by elongation of polar diagram of MT-34 and MT-35, especially at frequency 1 and 0.1 Hz.

Map of Identified Fault from MT Technology

The result of identified faults are plotted in a Map. The faults are inferred by analyzing curve splitting, 3D inversion, and polar diagram of MT data.

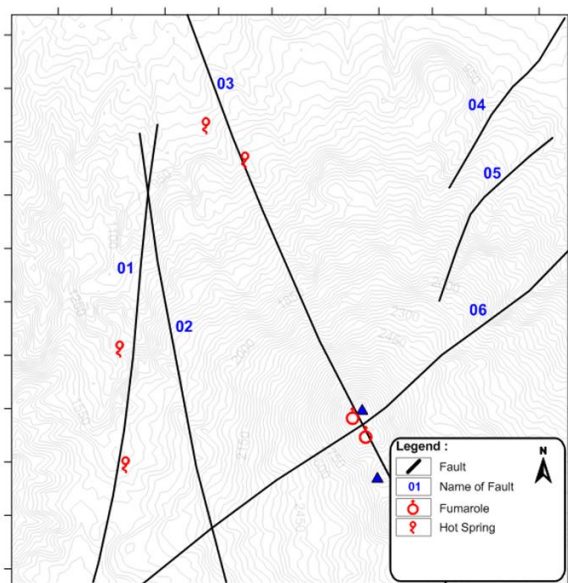


Figure 5. Map of identified faults

4. CONCLUSION

Continuation of Identified geological structure from field observation data to the subsurface is analyzed by using MT technology. The proposed technologies to characterize the subsurface geological structure are curve splitting, impedance polar diagram, and 3D inversion of MT data. Furthermore, this method has also been applied using real MT data from a geothermal area. MT data used to analyse the structure are divided to 4 profiles. From 7 analysed faults, 6 faults are identified using MT data and represented at structural map. However, further study of this method using real MT data and crosscheck by wellbore data from various geothermal area are needed to verify the reliability of this technology.

ACKNOWLEDGEMENT

The authors thank to Center for Geological Resources, Geological Agency, Indonesia for supporting in providing

geology and magnetotelluric data and for giving permission to publish these results. We are also grateful to Management of PT. NewQuest Geotechnology for providing 3-D MT data inversion software.

REFERENCES

- Daud, Y., Nuqramadha, W. A., Heditama, D. M., Fahmi, F., Pratama, S. A., & Hadi, J. (2015). Identification of Subsurface Geological Structure in A Geothermal System Using MT Imaging Technology. *World Geothermal Conference*. Melbourne.
- Daud, Y., Saputra, R., Heditama, D., & Nuqramadha, W. (2012). *MT3DInv-X: An Interactive 3-Dimensional Inversion of MT Data*. Internal Report of Collaboration between UI Geothermal Laboratory and PT NewQuest Geotechnology.
- Onacha, S. A., Shalev, E., Malin, P., & Leary, P. (2009). Joint Geophysical Imaging of Fluid-Filled Fracture Zones in Geothermal Fields in the Kenya Rift Valley. *GRC Transactions*.
- Onacha, S. A., Shalev, E., Malin, P., Arnasson, K., & Palsson, B. (2007). *Hydrothermal Fault Zone Mapping at Krafla Geothermal Field Using Seismic and Electrical Measurement*.
- Simpson, F., & Bahr, K. (2005). *Practical Magnetotelluric*. Cambridge University Press.
- Tong, L.-T., Ouyang, S., Guo, T.-R., Lee, C.-R., Hu, K.-H., Lee, C.-L., et al. (2008). Insight into the Geothermal Structure in Chingshui, Iilan, Taiwan. *Terr. Atmos. Ocean. Sci, Vol 19, No. 4*, 413-424.
- Ussher, G., Harvey, C., Johnstone, R., & Anderson, E. (2000). Understanding The Resistivity Observed in Geothermal Systems. *World Geothermal Congress*. Kyusu-Tohoku.
- Vozzof, K. (1991). The Magnetotelluric Method. Dalam M. N. Nabighian, *Electromagnetic Methods in Applied Geophysics - Applications Part A and Part B* (hal. 641 - 711). Society of Exploration Geophysicist.

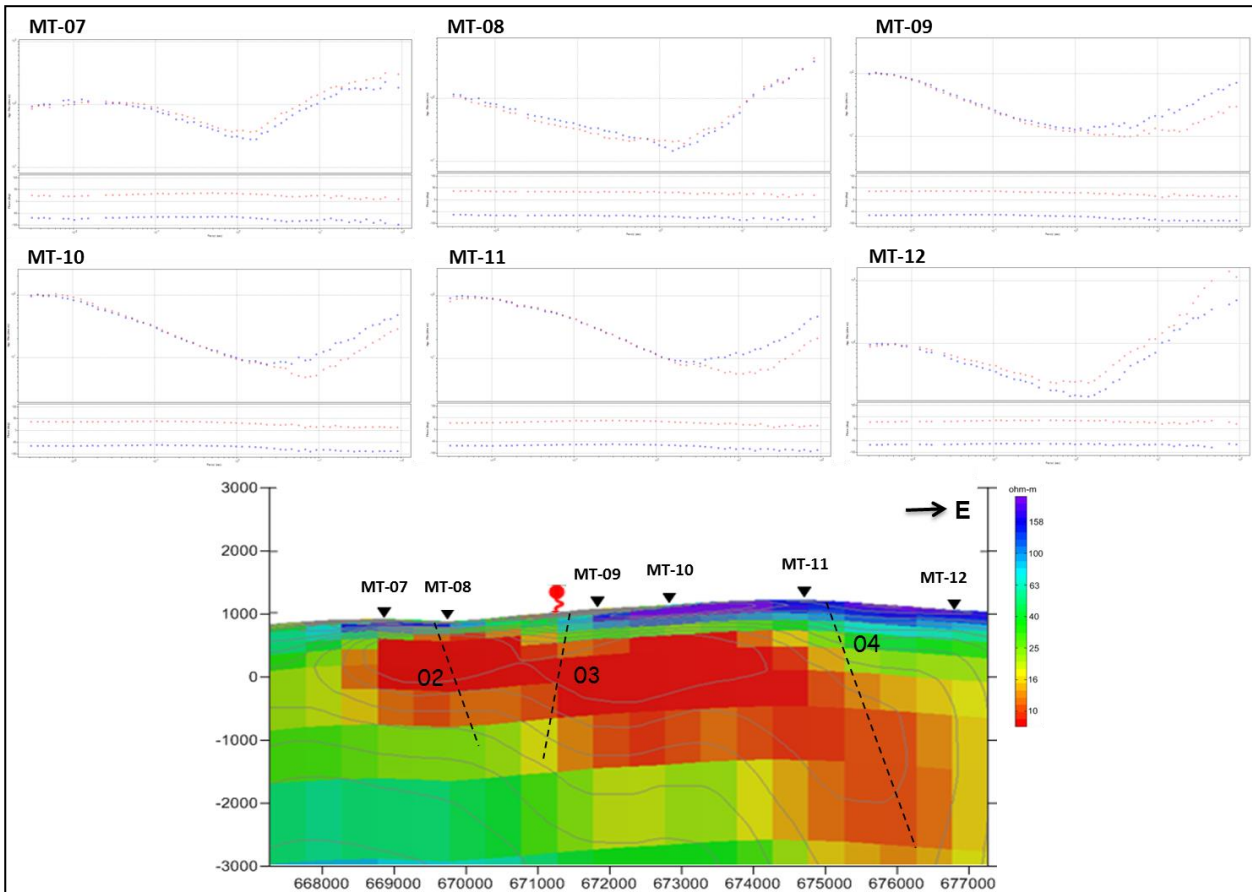


Figure 6. Curve splitting and 3D inversion result of Line 1

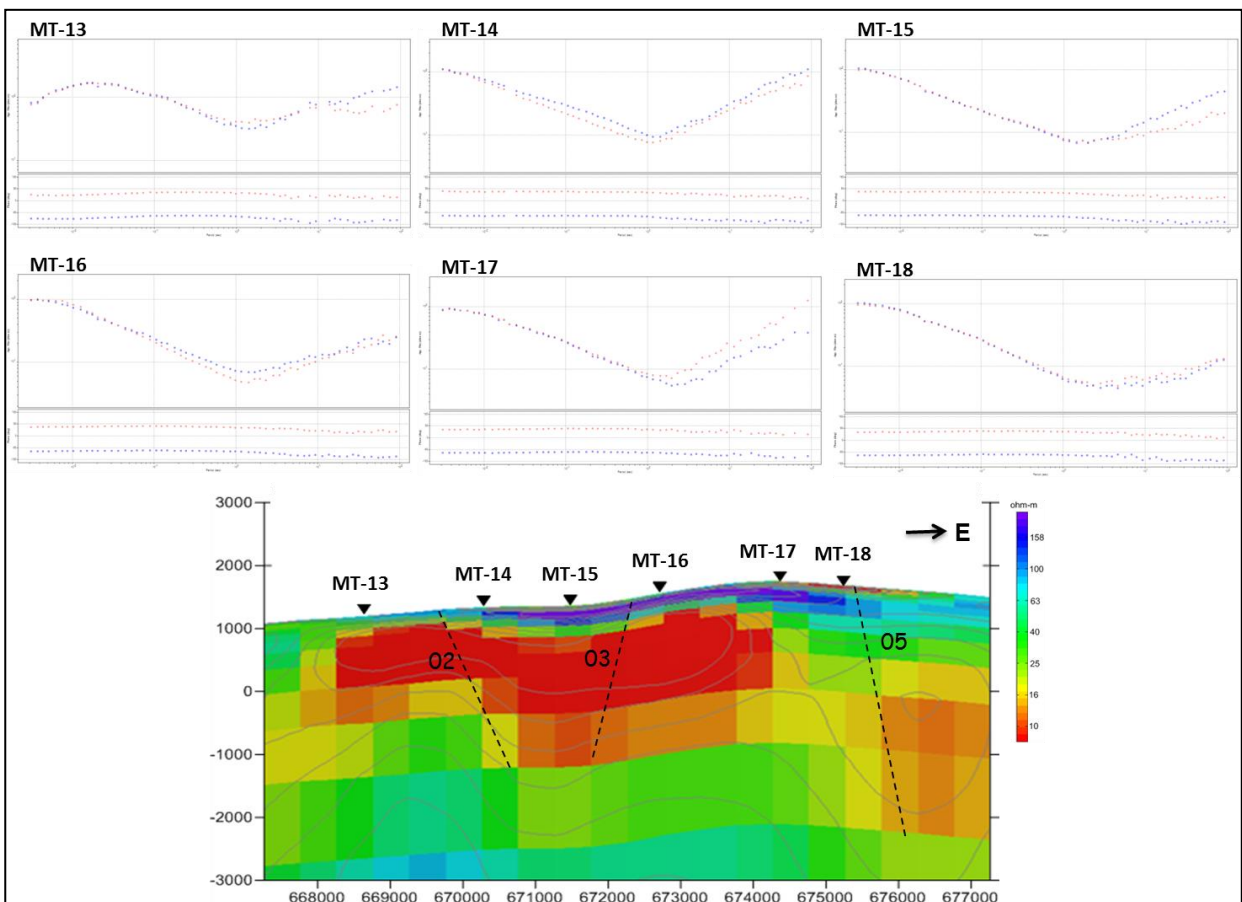


Figure 7. Curve splitting and 3D inversion result of Line 2

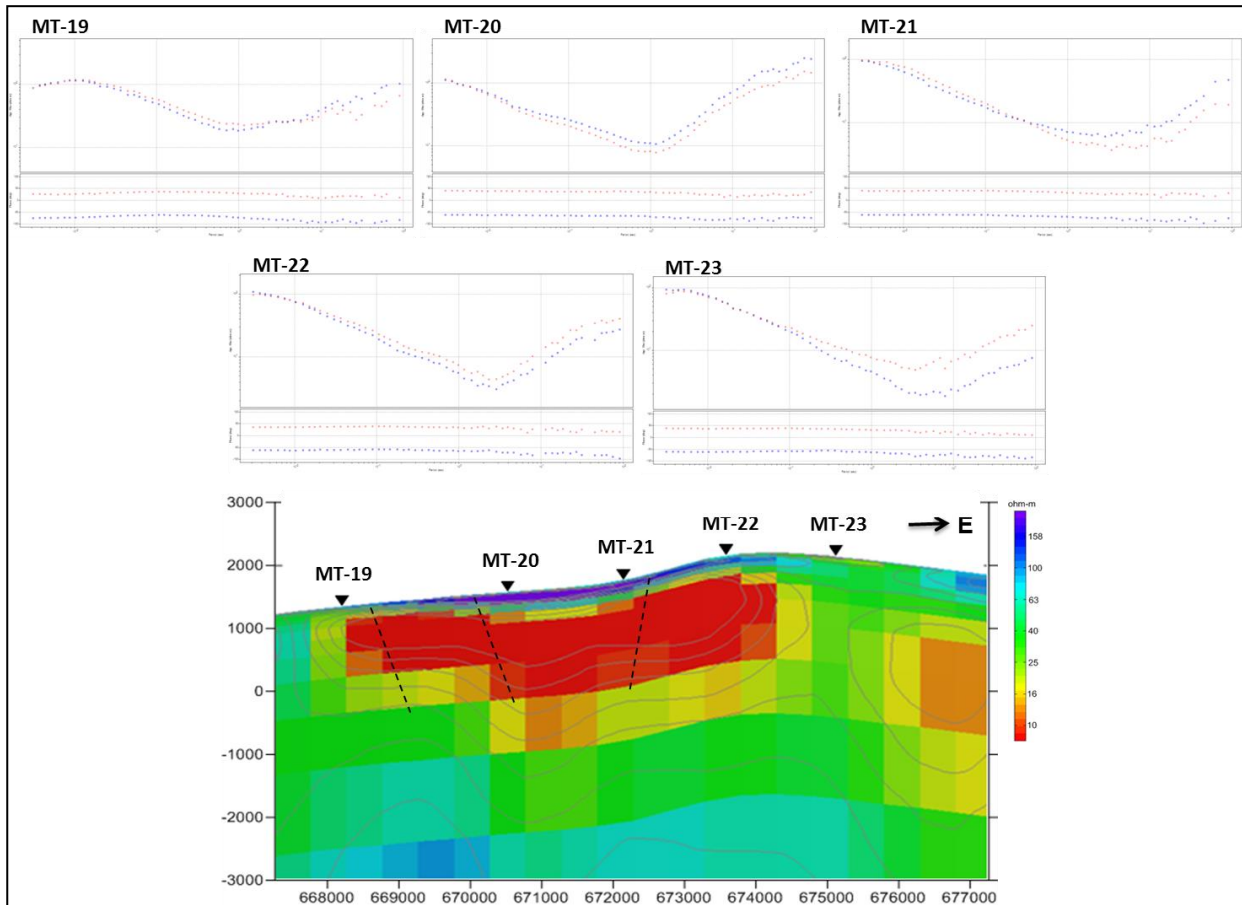


Figure 8. Curve splitting and 3D inversion result of Line 3

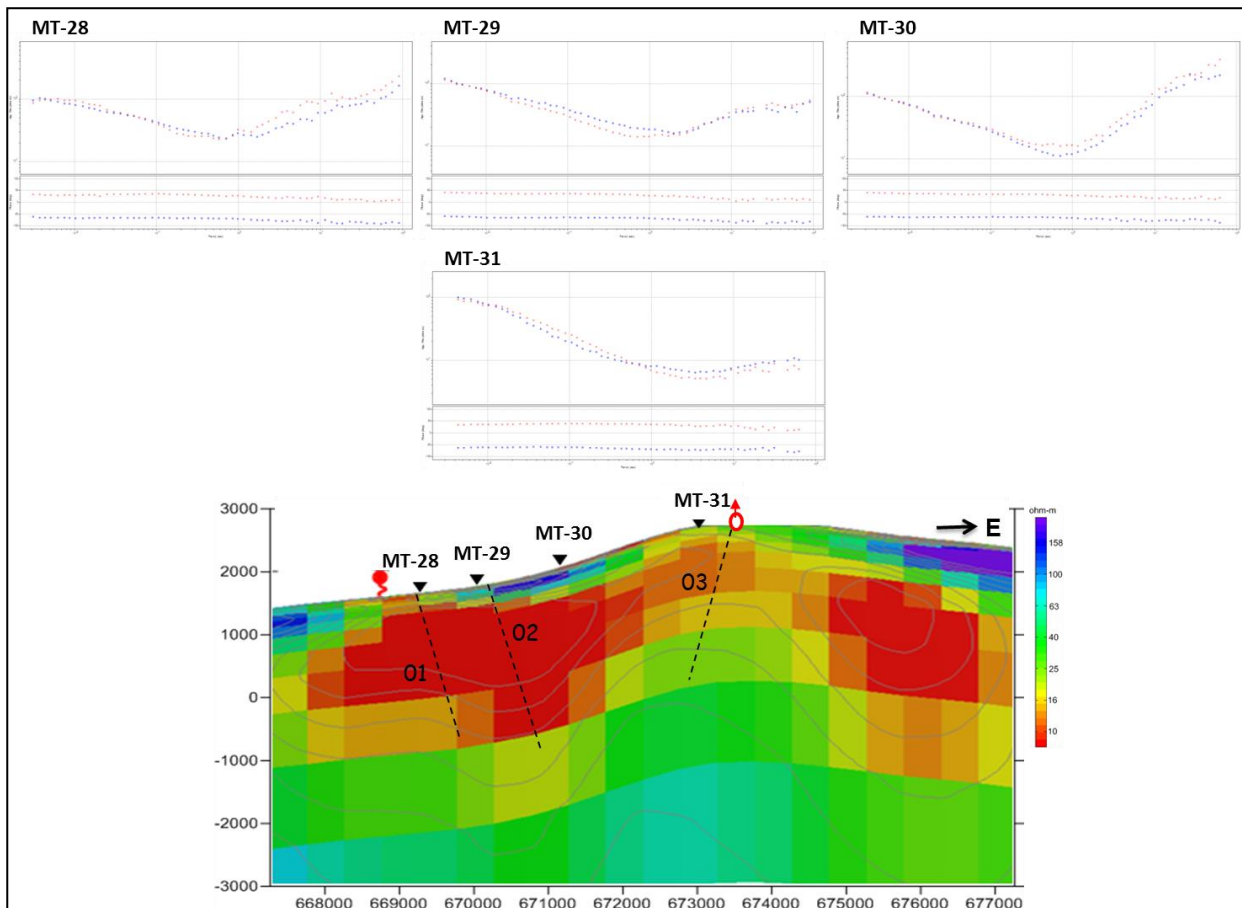


Figure 9. Curve splitting and 3D inversion result of Line 4

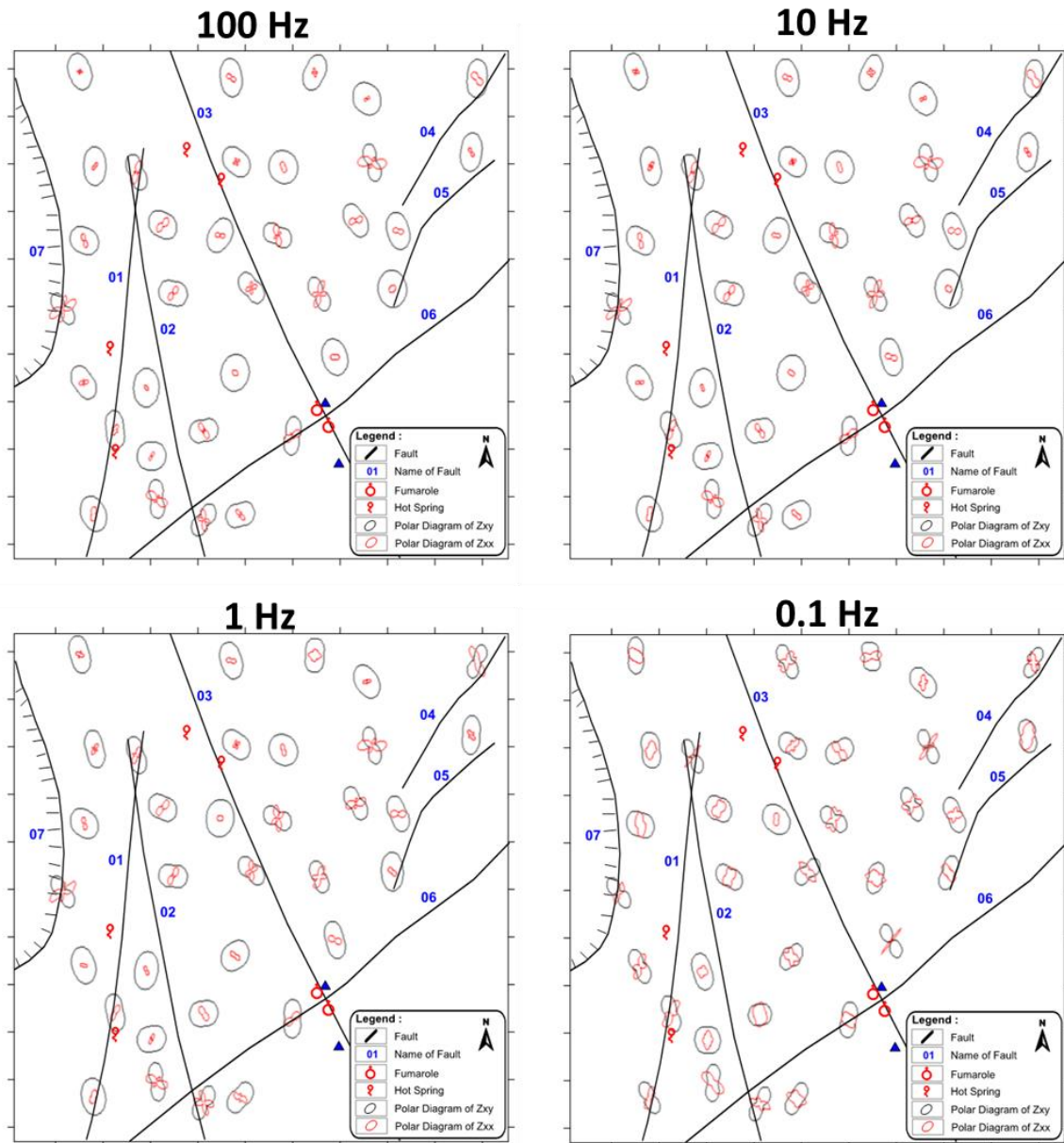


Figure 10. Polar diagram plotted at frequency 100, 10, 1 and 0.1 Hz